Published in final edited form as:
Sci Transl Med. 2014 September 24; 6(255): 255ra131. doi:10.1126/scitranslmed.3009701.

Coordinated Surgical Immune Signatures Contain Correlates of Clinical Recovery

Brice Gaudilliere[1,2,*], **Gabriela K Fragiadakis**[2,3,*], **Robert V Bruggner**[2,4], **Monica Nicolau**[5], **Rachel Finck**[2,3], **Martha Tingle**[1], **Julian Silva**[1], **Edward A Ganio**[1], **Christine G Yeh**[1], **William J Maloney**[6], **James I Huddleston**[6], **Stuart B Goodman**[6], **Mark M Davis**[3], **Sean C Bendall**[2,3], **Wendy J Fantl**[2,3], **Martin S Angst**[1,†], and **Garry P Nolan**[2,†]

[1]Department of Anesthesiology, Perioperative and Pain Medicine, Stanford University School of Medicine, Stanford, CA, USA

[2]Baxter Laboratory in Stem Cell Biology, Stanford University, Stanford, CA, USA

[3]Department of Microbiology and Immunology, Stanford University, Stanford, CA, USA

[4]Biomedical Informatics Program, Stanford University, Stanford, CA, USA

[5]Department of Mathematics, Stanford University, Stanford, CA, USA

[6]Department of Orthopedic Surgery, Stanford University, Redwood City, CA, USA

Abstract

Delayed recovery from surgery causes personal suffering and substantial societal and economic costs. Whether immune mechanisms determine recovery after surgical trauma remains ill-defined. Single-cell mass cytometry was applied to serial whole blood samples from 32 patients undergoing hip replacement to comprehensively characterize the phenotypical and functional immune response to surgical trauma. The simultaneous analysis of 14,000 phosphorylation events in precisely phenotyped immune cell subsets revealed uniform signaling responses among patients, demarcating a surgical immune signature. When regressed against clinical parameters of surgical recovery, including functional impairment and pain, strong correlations were found with STAT3, CREB and NF-kB signaling responses in subsets of $CD14^+$ monocytes ($R=0.7–0.8$, FDR < 0.01). These sentinel results demonstrate the capacity of mass cytometry to survey the human immune system in a relevant clinical context. The mechanistically derived immune correlates point to diagnostic signatures, and potential therapeutic targets, that could postoperatively improve patient recovery.

[†]These authors contributed equally and correspondence should be addressed to M.S.A. (ang@stanford.edu) and G.P.N. (gnolan@stanford.edu).
[*]These authors contributed equally to this work.

Author Contributions

B.G. and G.K.F. conceived the study, conducted experiments and wrote the manuscript. R.V.B., M.N. and R.F. developed and assisted in the implementation of computational methods for statistical data analysis. M.T. and J.S. assisted in patient recruitment and clinical data collection. E.A.G and C.G.Y. assisted in the fabrication of reagents and sample processing for mass cytometry analysis. W.J.M., J.I.H. and S.B.G. assisted in clinical study design and patient recruitment. M.M.D. and S.C.B. assisted in experimental design and interpreting data. W.F. assisted in interpreting data and writing the manuscript. M.A. and G.P.N. conceived and supervised the execution of the study, and wrote the manuscript.

Introduction

More than 100 million surgeries are performed annually in Europe and the United States (1). This number is expected to grow as the population ages. Convalescence after surgery is highly variable, and protracted recovery results in personal suffering, functional impairment, delayed return to work, and significant societal and economic costs (2). Recent work anchored in concept analysis defined postoperative recovery as the "process to regain control over physical, psychological, social and habitual functions, and return to preoperative levels of independence and psychological well-being" (3). This definition reflects a shift from traditional recovery parameters such as length of hospital stay, to patient-centered outcomes including absence of symptoms, the ability to perform regular activities, return to work, and regain quality of life (4). In this context, major determinants of protracted recovery are fatigue, pain and resulting functional impairment (5–7). Fatigue is a key sickness behavior and is described as "an indefinable weakness throughout the body requiring sitting or lying down after minor tasks".

Perioperative care now includes enhanced-recovery protocols and evidence-based practice guidelines largely anchored in observational data (8). While these protocols have reduced length of hospital stay, their impact on recovery after hospital discharge and the elements of these protocols that may contribute to improved recovery are uncertain. Similarly, the physiologic and mechanistic underpinnings of surgical recovery remain a "black box" phenomenon. Understanding the mechanisms that drive recovery after surgery will advance therapeutic strategies and allow patient-specific tailoring of recovery protocols. Considering that profound immune perturbations occur in response to surgery, comprehensive and longitudinal characterization of the human immune system in patients undergoing surgery is foundational for gaining such mechanistic insight.

Traumatic injury initiates an intricate programmed immune response (9): Hours following severe trauma, neutrophils and monocytes are rapidly activated and recruited to the periphery by damage-response antigens, alarmins (e.g., HMGB1), and increased levels of TNFα, IL-1β, IL-6 (10–13). This is followed by a compensatory phase characterized by decreased numbers of T cell subsets (13–16). The various immune cell types are thought to integrate multiple environmental signals into cohesive signaling responses that enable wound healing and recovery. A recent genome-wide analysis of pooled circulating leukocytes revealed that traumatic injury organized more than 80% of the leukocyte transcriptome according to cell type-specific signaling pathways (17).

The profound inflammatory response to tissue injury has prompted a long-standing interest in unraveling immune mechanisms that determine recovery after surgical trauma (18, 19). Previous studies have focused on secreted humoral factors (12, 20, 21), distribution patterns of immune cell subsets (11, 22), and genomic analysis of pooled circulating leukocytes (17, 23). These reports provided insight into aspects that govern the inflammatory response to traumatic injury but did not reveal strong correlations with clinical recovery. Although weak correlates to clinical outcomes were reported, none of these studies measured immune functional responses at the single-cell level, and strong signals might have gone undetected

as specific immune cell subsets would have been functionally and phenotypically under-characterized.

Here mass cytometry, a highly parameterized single-cell based platform that can determine functional responses in precisely phenotyped immune cell subsets (24–28), was employed to comprehensively characterize phenotypic and functional alterations of the human immune system as they occur *in-vivo*, in patients undergoing major surgery. The primary aim was to extract "surgery" or "trauma-specific" immune signatures and to determine, secondarily, whether such signatures contain clinical correlates of surgical recovery.

The expression levels of 35 cell-surface proteins and intracellular phospho-specific epitopes were simultaneously measured at 1 h, 24 h, 72 h, and 6 weeks after surgery in whole blood samples from an initial set of six patients, and then validated in a second set of twenty-six patients undergoing primary hip arthroplasty. Surface and intracellular markers were chosen to enable the comprehensive phenotyping of major immune cell populations (29) and the detailed examination of signaling pathways likely implicated in the immune response to traumatic injury, including the STATs, CREB and NF-κB signaling systems (9, 12, 17, 30). During a 6-week post-surgery observation period, functional recovery and resolution of fatigue and pain, the major determinants of clinical recovery, were evaluated every third day to infer individual patient's recovery profile at high temporal resolution (2, 5, 6, 31, 32). Highly regimented changes in the distribution of immune cells were observed in conjunction with cell-type specific signaling responses that demarcated a "trauma"-specific immune signature. When regressed against parameters of clinical recovery, strong correlates were found within signaling responses of specific cell subsets rather than in frequency changes of immune cell subsets. Notably, all signaling responses correlating with clinical recovery occurred in subsets of $CD14^+$ monocytes, underscoring the association of these cells with central processes enabling or disabling recovery from surgery.

Results

Mass cytometry enables the detection of surgery-induced immune perturbations in clinical samples

Based on a premise that surgical intervention, or "trauma", acts as a systemic perturbation on multiple physiologic processes in the body, cell subsets based on traditional surface marker phenotyping were analyzed simultaneously with intracellular signaling cascades downstream of activated receptors. Whole peripheral blood was collected from primary hip arthroplasty (PHA) patients and, critically, was processed within 30 minutes to remain as close as possible to *in-vivo* conditions. In a preliminary phase, samples from one patient collected 1 h before and 1 and 24 h after surgery were assayed in triplicate to determine whether trauma-induced changes in immune cell frequencies and intracellular signaling responses (phosphorylation of signaling proteins) could reliably be detected with mass cytometry (Fig. S1). The sensitivity and specificity of all phospho-specific antibodies used in the assay were validated *in-vitro*, in whole blood samples stimulated with a series of ligands known to induce the phosphorylation of signaling proteins included in the analysis (Fig. S1B). Reproducible changes were observed for cell frequencies and intracellular signaling responses, validating the assay for subsequent studies (Fig. S1).

In a pilot study of six PHA patients (Fig 1.), whole blood samples were collected 1 h before and 1 h, 24 h, 72 h, and 6 weeks after surgery. Samples were stained with antibodies recognizing 21 cell-surface proteins and phospho-epitopes of 10 intracellular proteins, and processed for mass cytometry (28) (Fig. 2A, Table S1). Significant effort was undertaken to protect against potential batch effect and minimize signal variation due to sample processing. Each time series was barcoded using a combination of stable isotope mass-tags (25) and processed simultaneously, and for each time point, reported frequencies and signaling responses were normalized to their measurements in the patient's baseline sample. Samples were also normalized for signal variation over machine-time using normalization beads containing known concentration of metal isotopes, as described in Finck *et al*. (33).

Analysis initially focused on neutrophils, $CD14^+$ monocytes ($CD14^+$MCs), and $CD4^+$ and $CD8^+$ T cells (Fig. S2, 3). Consistent with previous reports (11, 13, 15, 16, 34), surgery induced a 1.2-fold (±0.06, $q<0.01$) expansion of neutrophils 1 h after surgery, a 1.9-fold (±0.19, $q<0.01$) expansion of $CD14^+$MCs at 24 h, and a contraction of $CD4^+$ and $CD8^+$ T cells to 0.77-fold (±0.07, $q<0.01$) and 0.71-fold (±0.07, $q<0.01$), respectively, at 24 h (Fig. S3). Intracellular signaling responses, indicated by changes in phosphorylation of STAT1, STAT3, STAT5, CREB, and p38, were induced in time and cell-type specific manners (Fig. 2B, $q<0.01$). Six weeks after surgery, cell-subset frequencies and magnitudes of phospho-signals did not differ from pre-surgical values ($q>0.05$), indicating restoration of immune homeostasis.

$CD33^+CD11b^+CD14^+HLA\text{-}DR^{low}$ monocytes expand 6-fold after surgery

Having established that mass cytometry enabled the detection of surgery-induced perturbations in cell frequency and signaling, an observational study was conducted in twenty-six patients undergoing PHA to prospectively validate observed cellular responses to surgical trauma and to identify immune correlates of surgical recovery (Fig. 1, Table 1). All patients carried the primary diagnosis of non-traumatic osteoarthritis. Hip arthroplasties were performed using a standard lateral approach. Exclusion criteria included patients with any systemic disease or medication that might compromise the immune system (including recent infections, autoimmune disease, diagnosis of cancer, renal, hepatic, cardiovascular and respiratory disease resulting in functional impairment, history of substance abuse or chronic opioid therapy).

Serial blood samples and longitudinal data on clinical recovery were captured over a six-week period. Whole blood samples were barcoded, stained using the antibody panel in Fig. S1 (*right panel*) and processed by mass cytometry as described in the pilot study. The frequencies of neutrophils, $CD14^+$MCs, classical dendritic cells (cDCs), plasmacytoid dendritic cells (pDCs), natural killer cells (NK), B cells, and $CD4^+$ and $CD8^+$ T cells were determined by manual gating (29) (Fig. 3A, Fig. S2). Consistent with results from previous reports and the pilot study, NK cells (1.6-fold (±0.15, $q<0.01$)) and neutrophils (1.3-fold (±0.04, $q<0.01$)) expanded 1 h after surgery. $CD14^+$MCs expanded 2.4-fold (±0.29, $q<0.01$) and 1.8-fold (±0.16 $q<0.01$) at 24 h and 72 h, respectively. Mobilization of the myeloid compartment was followed by a contraction at 24 h of $CD4^+$ and $CD8^+$ T cells to 0.76-fold (±0.04, $q<0.01$) and 0.72-fold (±0.03, $q<0.01$), respectively, that became less pronounced at

72 h (0.88±0.04 and 0.85±0.03, respectively, $q<0.01$). Consistent with pilot results, cell-type frequencies six weeks after surgery were similar to pre-surgical values ($q>0.05$).

A major advantage afforded by high-dimensional multiparameter data analyses lies in the ability to detect finely tuned cell subsets with signaling changes that would be undetected in low parameter space. An unsupervised clustering algorithm was applied to comprehensively explore surgery-induced changes in cell subsets that may have been overlooked by manual gating strategies (35). The algorithm distills multidimensional single-cell data to a hierarchy of related clusters on the basis of cell surface markers (Fig. 3B, Fig. S4). Cluster-specific analysis of cell frequency changes revealed that clusters within the $CD45^+CD66^-CD3^-CD19^-CD33^+CD11b^+CD14^+$ compartment ($CD14^+$MC clusters) expanded 4-fold (±0.28) after surgery, more than any other cell cluster (Fig. S5). Expression of the HLA-DR antigen partitioned $CD14^+$MC clusters into HLA-DR^{hi}, HLA-$DR^{mid,}$ and HLA-DR^{low} compartments (Fig. 3C–G). Quantification of $CD14^+$MC cluster frequencies showed that the HLA-DR^{mid} and HLA-DR^{low} compartments accounted for 49% and 45% of the $CD14^+$MC cluster expansion (Fig. 3H–K). Notably, $CD33^+CD11b^+CD14^+$HLA-DR^{low} monocytes expanded 6-fold after surgery and had phenotypic similarity to myeloid derived suppressor cells (MDSC), previously described in the context of human malignancies as inhibitors of the adaptive immune system (36–38). Results of this unsupervised, high parameter analysis significantly expand previous reports on monocytic HLA-DR expression after surgery (39). The current results underscore an unequivocal role of HLA-DR^{mid} and HLA-DR^{low} $CD14^+$MCs in the surgical immune response as this approach enabled quantitative comparison among cell subsets within the broader context of the immune system.

STAT3, CREB and NF-κB signaling pathways are differentially activated in $CD14^+$ monocytes in response to surgery

A visual synopsis of surgery-induced changes in the phosphorylation states of eleven intracellular signaling proteins across eight different immune cell subsets, at four time points, and in 26 patients is shown (Fig. 4A). Significance Analysis of Microarray (SAM) (40) revealed 135 significant immune signaling responses to surgery ($q<0.01$) with cell-type specific distributions across major hematopoietic lineages (Fig. 4B). Notably, 97% of all phospho-signals detected 1 h before and 6 weeks after surgery were of similar magnitude ($q>0.05$), underscoring the tight regulation of the immune system and its ability to restore homeostasis (Fig. 4B).

Between 1 h and 72 h after surgery, time-dependent signaling responses were detected in all immune cell types (Table S2). Signaling changes were most pronounced in $CD14^+$MCs and $CD4^+$ T cells (Fig. 4B, Fig. S6). Sequential activation of STAT3 and STAT1 characterized the STAT response in $CD14^+$ MCs, whereas activation of STAT3 and STAT5 characterized the STAT response in $CD4^+$ T cells. Activation of STAT3 and STAT5 in $CD4^+$ T cells was detected at 1 h; the highest level of activity of STAT3 in $CD14^+$MCs was observed at this time point. Activity of STAT3 and STAT5 was less pronounced in $CD8^+$ than $CD4^+$ T cells but followed a similar pattern. Results indicate early and concurrent activation of major signaling pathways in innate and adaptive immune cell compartments. This challenges the

conventional view that innate and adaptive immune responses to surgical trauma follow a sequential temporal pattern (18).

Further investigation of signaling responses in $CD14^{+}$MCs revealed significant de-phosphorylation of ERK, p38, MAPKAPK2, p90RSK, rpS6, CREB, and NF-κB (p65-RelA) at 1 h after surgery (Fig. 4A, 4B and Fig. S6). By 72 h, phosphorylation of these proteins had either returned to or exceeded baseline values. To characterize the signaling network underlying these coordinated phosphorylation patterns, correlation analysis was performed (Fig. 4C). Clustering of the resultant correlation coefficients revealed four modules that were preserved in all patients at all time points after surgery (Fig. 4D, 4E and Fig. S7). Module 1 consisted of pNF-κB, pCREB, and prpS6, and module 2 consisted of pp38, pMAPKAPK2, pERK, and pp90RSK. Each of these proteins can be activated downstream of Toll-like receptors known to play an essential role in the innate response to sterile inflammation (41, 42). Module 1 also included STAT1, possibly reflecting the indirect regulation of STAT1 downstream of TLR4 (43). Module 3 consisted of pSTAT5 and pPLCγ2, suggestive of coordinated activations of parallel signaling pathways not previously shown to cross-communicate (44, 45), which warrants further investigation. Module 4 consisted only of pSTAT3 and was anti-correlated with other modules; the pSTAT3 response may be linked to the known increase in plasma IL-6 concentration after surgery (12).

Considering that the inflammatory response to surgical trauma can engage as many as 40 receptors including receptors for alarmins (such as TLR 2 and 4), interleukin receptors and others (9, 10), the consistent integration of multiple environmental signals into cell type-specific signaling networks highlights the ability of the immune system to mount a uniform surgical immune response. The magnitude of this response varied among patients, which begs the question as to whether the variability between patients constitutes “noise” or, alternatively, reflects patient-specific differences that could correlate with differences in clinical recovery.

Dense longitudinal characterization of clinical recovery reveals large inter-patient variability

Fatigue, pain and resulting functional impairment after surgery critically determine when patients can resume normal activities and return to work (5, 6, 32). Fatigue, pain and functional impairment of the hip were assessed with the Surgical Recovery Scale, and adapted versions of the Western Ontario and McMaster Universities Arthritis Index (WOMAC) pain and function sub-scales. Assessments were obtained daily during hospitalization, and then every third day up to six weeks to infer the rate at which individual patient’s recovered from surgery. Rates were quantified as the time required to reach half maximum recovery from fatigue, to transition from moderate to mild pain, and to transition from moderate to mild functional impairment of the hip; all considered to be clinically important milestones in a patient’s recovery.

Heat maps depicting parameters of clinical recovery for individual patients during the six-week period following surgery reflect large inter-patient variability for the three outcomes: fatigue, hip function, and pain (Fig. 5A–C). The median time to recuperate from

postoperative fatigue was 3 weeks. Clinical resolution of significant functional impairment of the hip (score ≤18) and pain (score ≤12) occurred during the second week (Fig. 5D–F). However, the rate of recovery varied greatly among patients. The median time to regain 50% of recovery from postoperative fatigue was 10 days with a range of 0 to 36 days. The median time to experience only mild functional impairment of the hip was 15 days with a range of 2 to 42 days. The median time to suffer from only mild pain was 10 days with a similar wide range of 2 to 36 days (Fig. 5G–I). Among all demographic and clinical variables only gender was significantly related to a clinical recovery parameter. The median time to regain 50% recovery from postoperative fatigue was 6 days (range 5–12) in women and 15 days (range 6–20) in men (p=0.02). Recovery of postoperative fatigue was not correlated with times to mild functional impairment of the hip or pain, but a significant correlation was detected between the times to mild functional impairment of the hip and pain (R=0.6, p=0.004). Thus, in this homogeneous patient population rates of recovery differed greatly.

Signaling responses in CD14^{+} monocyte subsets correlate with surgical recovery

To gain an objective view of the relationships between the multidimensional mass cytometry dataset and clinical outcomes, a method for unsupervised identification of cellular responses associated with a clinical outcome was used (35) (Fig. 6A). This algorithm demarks cell subsets using the hierarchical clustering described above (Fig. 3), attributes immune features (cell frequencies and signaling responses) to each cell cluster, and identifies significant associations ($q<0.01$) between immune features and parameters of clinical recovery using SAM. Significant correlations were detected for six immune cell features at a false discovery rate of 1% (R = 0.66–0.80, Table 2). All were signaling responses in CD14^{+}MC subsets (Fig. 6B, 6C). For instance, changes in STAT3 signaling between 1 h and 24 h in CD14^{+}HLA-DR$^{low/mid}$ MC clusters strongly correlated (R=0.72–0.80) with time to 50% recovery from postoperative fatigue (Fig. 6B, panel 1, Fig. S8). Changes in CREB signaling between baseline and 1 h in the CD14^{+}HLA-DR^{low} MC cluster strongly correlated (R=0.66) with time to mild functional impairment of the hip (Fig. 6B, panel 2). Changes in NF-κB signaling between baseline and 1 h in the CD14^{+}HLA-DR^{hi} MC cluster strongly correlated (R=0.71) with time to mild pain (Fig. 6B, panel 3). These correlations remained significant and unchanged when accounting for potential confounders (including sex, age, BMI, type of anesthesia, duration of surgery and estimated blood loss, Table S3) and were confirmed by a manual gating strategy (Fig. 6C, 6D). Since analgesic consumption and pain are interrelated factors, a quantitative analysis accounting for confounding influences of post-operative analgesic consumption on pain was performed (46). Variation in analgesic consumption did not alter the correlation between NF-κB signaling in CD14^{+}HLA-DR^{hi} MCs and time to mild pain. Thus, specific signaling responses in monocyte compartments are hallmarks of critical phenotypes defining clinical recovery and account for 40–60% of observed inter-patient variability.

Discussion

This study applied mass cytometry to survey with single-cell resolution the phenotypical and functional alterations of the human immune system in patients undergoing major surgeries,

namely hip arthroplasty. Simultaneous assessment of immune cell distributions and corresponding intracellular signaling events revealed uniform responses across patients, thereby demarcating a surgical immune signature. Engrained in this immune signature were strong correlates (R=0.7–0.8, FDR<0.01) relating the magnitude of cell-type specific signaling responses to an individual patient's clinical recovery profile.

Mass cytometry provided high-dimensional numerical and functional characterization of the immune response to surgical trauma and enabled the detection of biological mechanisms critically associated with a health-relevant outcome. Using an unsupervised algorithmic approach changes in cell frequencies and immune signaling responses at the single cell level were systematically evaluated via deep immune system profiling to identify immune correlates of clinical recovery. Two themes evolved: 1) strong correlations were identified with signaling responses but not with changes in cell frequency and 2) signaling responses that correlated most significantly with clinical recovery occurred in $CD14^+$ monocytes. These included changes in STAT3, CREB and NF-κB activation states within $CD14^+$ monocyte subsets, which correlated with recovery from fatigue, functional impairment of the hip and pain after surgery and accounted for 40–60% of observed patient variability.

The simultaneous monitoring of major immune cell subsets provided a global view of surgery-induced alterations across the immune system that included precisely timed changes in immune cell distribution and mobilization of distinct signaling networks in innate and adaptive compartments. Consistent with previous studies (11, 13–15, 34, 47), innate immune cells expanded soon after surgery, followed by a reduction of cells within the adaptive branch (Fig. 3). In contrast, cell-signaling responses occurred early and simultaneously within both immune branches (Fig. 4). For instance, orchestrated changes in STAT3 and STAT5 signaling manifested within 1 h after surgery in $CD14^+$MCs and $CD4^+$ and $CD8^+$ T cells. Our results challenge the view that innate immune responses to trauma precede adaptive responses. For instance, it raises the question of whether adaptive immune cells might migrate to sites to prepare for events driven by innate processes. Our data dovetail with findings of a recent genome-wide analysis of the leukocyte response to major trauma (17). In that study, up-regulation of genes associated with the innate immune branch and those encoding pro-inflammatory mediators, including STAT target genes, was concurrent with the suppression of genes associated with the adaptive immune branch including genes regulating T cell proliferation, antigen presentation, and apoptosis.

In $CD14^+$ monocytes, STAT3 phosphorylation peaked 1 h after surgery in all patients and coincided with the de-phosphorylation of 10 signaling proteins, which formed four distinct modules (Fig. 4). The observed activation of STAT proteins in $CD14^+$ monocytes within 24 h after surgery is consistent with previously reported trauma-induced increases in plasma cytokine IL-6 (12) and IL-10 (48, 49), a key response to trauma. Unexpectedly, a biphasic response of several signaling pathways downstream of Toll-Like Receptors, which play a major role in innate immunity (41, 42), was observed (Fig. 4). This might be due to the release of trauma induced signaling molecules such as HMGB-1, Heat Shock Proteins and other alarmins known to act on Toll-Like Receptors and other immune mediators of inflammation (9, 30). The coordinated and sequential de-phosphorylation and phosphorylation of these proteins is reminiscent of oscillations in NF-κB nuclear

translocation, which control the expression of NF-κB target genes (50). Oscillations in CREB and NF-κB signaling networks together with STAT3 signaling may drive the response of $CD14^+$ monocytes to surgical trauma.

Observed similarities in signaling activities among patients are indicative of a tightly regimented immune response to surgical trauma. We hypothesized that the differences in the magnitude of such responses may account for differences in recovery from surgery. Indeed, inter-patient variability in phosphorylation of proteins within two signaling modules in $CD14^+$ monocytes, those involving STAT3 (Module 4) and CREB and NF-κB (Module 1) (Fig. 4), strongly correlated with recovery from postoperative fatigue and resolution of pain after surgery, suggesting that differential engagement of these signaling networks in $CD14^+$ monocytes regulate important aspects of clinical recovery (Fig. 6).

The most significant immune correlates of clinical recovery occurred in $CD11b^+CD14^+HLA\text{-}DR^{low}$ monocytes (Fig. 6). A marked over-representation of this cell subset was observed at 24 h and 72 h after surgery (Fig. 3). An explanation that could account for this observation is the down-regulation of HLA-DR expression, a proposed mechanism of "monocytic anergy" after major trauma and sepsis (51–53). However, phenotypically the $CD11b^+CD14^+HLA\text{-}DR^{low}$ monocytes we observed are remarkably similar to that reported for myeloid derived suppressor cells (MDSCs), which dramatically expand in a mouse model of surgery (54). In human malignancies $CD11b^+CD14^+HLA\text{-}DR^{low}$ MDSCs proliferate and suppress T cell responses in a STAT3-dependent fashion (37, 55). The observed preponderance of $CD11b^+CD14^+HLA\text{-}DR^{low}$ cells after surgery and the strong correlation between STAT3 signaling in these cells and patients' fatigue suggests that these cells might play an important role in regulating critical aspects of clinical recovery.

Previous studies had revealed a link between surgery-related inflammatory responses and clinical recovery; however, the immune features only explained a small fraction of variability in recovery rates and provided limited mechanistic insight. For example, Hall *et al*. detected a correlation between IL-6 plasma concentrations at 24 h after hip replacement and the time after surgery when a patient was able to walk 25 meters (56). Rosenberg *et al*. found a correlation between leukocyte redistribution from the blood stream and joint function after surgery in patients undergoing knee replacement (11). By contrast, the study presented here revealed highly specific immune correlates accounting for 40–60% of variability in recovery rates (Fig. 6). Prior studies that relied on bulk analysis, precluded detailed sub-setting of cells, or could not measure functional attributes of rare cell subsets may have missed strong correlative signals. Notably, in our study, signaling responses in less than 2% of peripheral leukocytes correlated with a given clinical correlate.

The role of the immune system in recovery after surgery or major trauma remains elusive. At first consideration, it seems clear that a battle-ready immune system must be mobilized at the first sign of injury to ensure efficient pathogen defense, wound-healing, and tissue regeneration (9, 57, 58). Complications, such as infections, protracted wound-healing and delayed recovery may arise when the immune system is off-balance and fails to effectively regulate the inflammatory response to traumatic injury. The studies here suggest that cellular events can be identified that reflect a maladaptive immune response, which hinders recovery

from surgery. For example, sustained STAT3 and CREB activities in HLA-DR^{low} CD14^{+} monocyte subsets strongly correlated with protracted postoperative fatigue and impaired hip function. Observations of such robust immune correlates imply that characterizing these cellular events can guide the identification of effector mechanisms which directly regulate maladaptive inflammatory processes associated with impaired surgical recovery. Whether these cell subsets and their cognate signaling events are causative or are downstream hallmarks of surgical recovery remains to be determined.

This study has certain limitations. The patient cohort, while homogenous, suffered from minimal co-morbidities and underwent the same surgical procedure (Table 1), which enabled the identification of key immune correlates of recovery from hip surgery. These results may not extrapolate to all types of surgery or trauma, but the highly structured immune response observed in these patients suggests that reported immune signatures might be generalizable. Our study was therefore designed to ask “what were the baseline immune correlates for this type of surgery”. We expect of course that co-morbidities might introduce additional variations specific to the co-pathology. The immune correlates of clinical recovery were derived from the analysis of samples collected within 72 hour after surgery, leaving open the possibility that other important and identifiable events may occur later in the recovery phase. This study used simultaneous assessment of 35 parameters per single-cell. However, in the near future it will be possible to measure 70 parameters per cell (G Han, GPN unpublished), which will allow more comprehensive characterizations of cell subsets and signaling networks vis-a-vis their role in clinical recovery. Finally, while the relevant signaling events identified in the pilot study were subsequently validated in a 26-patient cohort, the predictive value of observed clinical recovery correlates will require prospective validation in an independent patient cohort.

The role of monocytes in surgical recovery and trauma has been subject of significant interest (39, 52, 59–63). Application of single cell analysis at the bedside enabled identification of strong and specific immune correlates in CD14^{+} monocytes that accounted for 40–60% of patient-associated variability in recovery after PHA. Importantly, immune correlates pertained to the functional (i.e., signaling) state of CD14^{+} monocytes rather than their frequency. These data therefore provide a first set of mechanistically based targets in immune cells, such as monocytes, that can be exploited to advance post-operative care in surgical patients.

Materials and Methods

Experimental Design

Subjects—The study was approved by the Institutional review Board of Stanford University School of Medicine and registered with ClinicalTrials.gov (NCT01578798). Patients scheduled for primary hip arthroplasty for non-traumatic osteoarthritis were recruited from the Arthritis and Joint Replacement Clinic in the Department of Orthopedic Surgery at Stanford University School of Medicine. Hip arthroplasties were performed by one of three surgeons using a standard lateral approach, wound drains and compression dressings. Patients were mobilized early after surgery (day of surgery) and the bladder catheter was removed on postoperative day 2. Hospital discharge was planned for

postoperative days 3–4. A total of 251 patients were screened, 81 were approached for informed consent, 50 were consented, 39 were actively enrolled, and 32 completed the study (Fig 1., Table 1). Inclusion criteria were: 1) scheduled for primary hip arthroplasty, 2) age 18–90 years, 3) fluent in English, and 4) willing and able to sign informed consent and the Health Insurance Portability and Accountability Act (HIPAA) authorization. Exclusion criteria were: 1) any systemic disease or medication that might compromise the immune system, 2) diagnosis of cancer within the last 5 years, 3) psychiatric, immunological, and neurological conditions that would interfere with the collection and interpretation of study data, 4) pregnancy, and 5) any other conditions that, in the opinion of the investigators, may have compromised a participant's safety or the integrity of the study (including history of substance abuse, chronic opioid therapy >30mg/day, infectious disease within 1 month, and renal, hepatic, cardiovascular and respiratory disease resulting in functional impairment). Given the exclusion criteria comorbidities were minor and included clinically compensated atrial hypertension (11), diabetes mellitus (2), hypothyroidism (1), and asthma (1).

Study protocol—Assessments were made 1 h before and 1, 24, 48, and 72 h after surgery and every third day from day 6 to day 42. Clinical outcomes were captured with the Surgical Recovery Scale (SRS; 0–100 = worst/best function), an adapted Western Ontario and McMaster Universities Arthritis Index (WOMAC) pain scale (WOMAC-P; 0–40 = no/worst imaginable pain), and an adapted WOMAC function scale (WOMAC-F; 0–60 = no/severe functional impairment). Adapted versions were used because not all questions applied to the postoperative setting. Daily opioid consumption was captured as intravenous hydromorphone equivalents. Full versions of the WOMAC, the Short Form Health Survey (SF-36), the Profile of Moods States Tension-Anxiety Scale (POMS-A) and the Beck Depression Inventory (BDI) were completed at the beginning and end of the study (64–67).

Clinical data—Results are presented as medians and interquartile ranges. Recovery from postoperative fatigue (SRS) was quantified as the time required to half maximum recovery (SRS-$t_{1/2}$), defined by a surgical recovery index (SRI) equivalent to the sum of the minimum SRI after surgery and half of the difference between the preoperative SRI and the minimum SRI. SRS-$t_{1/2}$ was more sensitive than time to full recovery as the latter parameter was affected by ceiling effects.

Recovery from pain was quantified as the time required to achieve a WOMAC-P ≤ 12 (T_{12}). WOMAC-P was composed of four scores (0–10 = no/most imaginable pain) to quantify pain at night, at rest, when bearing weight, and during walking. A cumulative score of 12 indicates transition from mild to moderate pain across the conditions (68).

Recovery of hip function was quantified as the time required to achieve a WOMAC-F ≤ 18 (T_{18}). WOMAC-F was composed of six scores (0–10 = no/severely impaired) to quantify function in the affected hip when lying in bed, rising from bed, sitting, rising from sitting, standing, and walking on flat surface. A cumulative score of 18 indicates transition from moderate to mild functional impairment across the conditions.

Patient Sample Processing by Mass Cytometry

Whole blood processing—Blood samples were resuspended in stabilizing buffer (Smarttube, Inc.) within 30 min of phlebotomy and stored at −80 °C. Samples were thawed on the day of processing. Red blood cells were lysed using a hypotonic buffer. Peripheral blood leukocytes were washed and resuspended in cell staining media.

In vitro stimulation of whole blood samples—Stimulations were performed for antibody validation (Fig. S1B). Samples were incubated with PBS, interleukin cocktail (100 ng/mL IL-2 [BD Biosciences]; 100 ng/mL IL-6 [BD Pharmingen]; 20 ng/mL IFNα [Sigma-Aldrich]; 2 ng/mL GMCSF [PeproTech]), 80 nM phorbol 12-myristate 13-acetate/1.3 μM ionomycin, [Ebioscience]), or 0.5 mM activated sodium orthovanadate [Calbiochem]) for 15 min at 37 °C. Blood samples were resuspended, cooled to 4 °C and stored at −80 °C.

Antibodies—Antibodies were chosen to facilitate the identification of major immune cell types in whole blood (Fig. S2) as well as to measure immune signaling pathways likely to be affected by surgery. The antibodies used for the six-patient pilot study are listed in Table S1, a subset of these were used for experiments described in Fig. S1. An updated panel (Table S1) was used for the 26-patient study. This panel substituted signaling antibodies that showed little change in the six patients (pSTAT4, pSTAT6) with antibodies that reflected pathways that changed more substantially (pMAPKAPK2, pP90RSK, pNF-κB (p65-RelA)). Phenotypic antibodies were updated by substituting non-functional or redundant markers (CD20, CD27) with markers that facilitate the gating of additional cell populations (CD25, CD127, NkP44, CD69, FoxP3).

A subset of the antibodies was obtained pre-labeled by DVS Sciences (DVS Sciences); others were metal-labeled as described by Bendall *et al*. (28). Briefly, antibodies were obtained in carrier protein-free PBS and labeled using the MaxPAR antibody conjugation kit (DVS Sciences) according to the manufacturer's protocol. All metal-labeled antibodies were diluted based on their percent yield by measurement of absorbance at 280 nm to 0.2 mg/mL in Candor PBS Antibody Stabilization solution (Candor Biosciences) for storage at 4 °C.

Barcoding—Reagents were prepared according to the procedure described in Bodenmiller *et al*. (25). Two molar equivalents of maleimido-mono-amide-DOTA (Macrocyclics, Inc.) were added to palladium 102, 104, 105, 106, 108, 110, each contained in 20 mM ammonium acetate at pH 6.0. Solutions were immediately lyophilized, and solids were dissolved in dimethyl sulfoxide (DMSO) to 10 mM for storage at −20 °C. Each well of a barcoding plate contained a unique combination of three palladium isotopes at 200 nM in DMSO.

Cell barcoding and antibody staining—Time points from the same patient (BL, 1 h, 24 h, 72 h, 6 weeks) were barcoded and processed simultaneously. Therefore, each of a given patient's time points was subjected to identical processing, such that there was no systematic experimental bias applied to a given time point across patients. To protect against potential batch effects, all findings are quantified as relative changes between time points (i.e. all reported values are normalized to a signal from its same barcode plate). Machine-based batch effects were normalized post processing (33).

All decisions regarding which patients were barcoded together, and all staining, mass cytometry analysis, and quantification of changes was performed blinded to the patients' recovery status. In addition immune features used for regression against recovery were derived blinded to recovery indices.

Cells were barcoded with alterations for pre-permeabilization (25). Cells were transferred into a deep-well block and washed once with Cell Staining Media (CSM, PBS with 0.5% BSA, 0.02% NaN_3), once with PBS, then once with 0.02% saponin in PBS leaving cells in 100μL residual volume. The barcoding plate was thawed on ice, and 1 mL 0.02% saponin/PBS was added to each well. Aliquots were transferred to cells, and samples were incubated at room temperature for 15 min, washed twice with CSM, and pooled into one FACS tube for staining with metal-labeled antibodies.

Cells were washed once with CSM and then incubated for 10 min at room temperature with one test of FcX block (Biolegend) to block non-specific Fc binding. Cells were stained with the surface antibody cocktail for 30 min and washed once with CSM. Cells were permeabilized with 1 mL of methanol for 10 min on ice. Cells were washed twice with PBS and once with CSM and incubated with the intracellular antibody cocktail for 30 min at room temperature. Cells were washed once with CSM then incubated overnight at 4 °C with an iridium-containing intercalator from DVS Sciences in PBS with 1.6% formaldehyde. Cells were washed twice with CSM, once with water, and then resuspended in a solution of normalization beads as described by Finck *et al*. (33). Cells were filtered through a 35-μm membrane prior to mass cytometry analysis.

Mass cytometry—Stained cells were analyzed on a mass cytometer (CyTOF, DVS Sciences) at an event rate of 400–500 cells per second. Data files for each barcoded sample were concatenated using an in-house script. The data were normalized using Normalizer v0.1 MCR (33). Files were de-barcoded using the Matlab Debarcoder Tool. Gating was performed in nolanlab.cytobank.org (Fig. S2).

Mass cytometry data processing—An inverse hyperbolic sine transformation was applied to analyze protein phosphorylation data. The difference of the median of the transformed values between baseline and 1 h, 24 h, 72 h, and 6 weeks after surgery is reported as the arcsinh ratio.

Statistical Analysis

Sample size determination for the validation of surgery-induced signaling events—A power analysis was anchored in the pilot data (6 patients, Fig. 1). Considering all signaling responses with arcsinh ratios equal or greater than 0.2, the response associated with the highest variance (pp38 in $C14^+$MCs) was used to determine power. Assuming an alpha level of 0.001, a sample size of 24 patients would allow detecting this signaling response with a power of 90%.

Statistical analyses of molecular parameters—Significant changes in cell frequency and phosphorylation state were inferred with SAM_ENREF_34 (40), using the "samr" package in R. SAM is a non-parametric test that assigns a score to the change in each

feature, and thresholds that score for significance based on an estimate of FDR derived from permuting the observed data. This test was selected because it corrects for multiple-hypothesis testing, makes few assumptions about the distribution of the underlying data, and has been validated for use on high dimensional biological data. SAM Two class paired was performed for hand-gated data. Significance was inferred for a false discovery rate <1% (FDR, $q<0.01$).

Correlation network analysis—Monocyte signaling responses from all time points were used to generate a Pearson correlation matrix, which was clustered using single-linkage clustering (Fig. S7). Clusters were collapsed into a module when the within-cluster correlation exceeded 0.7 (Fig. 4D). Correlations between two modules were calculated as the average of the correlation between the points in the two modules (Fig. 4E).

Clustering—Hierarchical clustering using Ward's linkage and Euclidean distance was performed as described in Bruggner *et al*. (35), on $CD45^{+}CD66^{-}$ cells using R (Fig. 3, Fig. 6). Cells were clustered based on the expression of CD7, CD19, CD11b, CD4, CD8, CD127, CCR7, CD123, CD45RA, CD33, CD11c, CD14, CD16, FoxP3, CD25, CD3, HLA-DR, and CD56. Ten thousand events were sampled from each patient sample for clustering. Clusters containing at least 1% of all clustered cells are graphically displayed. Data from time-points that were included in the same SAM analysis were clustered together to enable comparison of clusters between time-points.

Correlation analyses of molecular and clinical parameters—Correlation analyses of molecular features derived from mass cytometry data and clinical parameters were performed using Citrus, a method for unsupervised identification of cellular responses associated with a clinical outcome (35). Briefly, cell subsets were identified using hierarchical clustering as described in the "clustering" section. Cells from each patient and from each time point were pooled for clustering to enable comparison across samples. For each cluster in each patient, cluster abundances and the median value of 11 phospho-proteins were calculated as relative changes between time points to avoid potential batch effects. Associations between clinical endpoints and cluster properties were identified using the SAM Quantitative method. Repeated runs of the analysis with identical parameters confirmed that results were reproducible.

Partial correlation was performed by correlating the residuals from (1) the correlation of the clinical covariate with the immune feature and (2) the correlation between the clinical covariate and the clinical index. Clinical covariates included age, sex, BMI, estimated blood loss, length of surgery, use of regional anesthesia, and baseline clinical indices of recovery. Analysis was performed in the R software environment. P-values from this analysis were compared to the p-values for the immune feature correlation with the clinical index and are listed in Table S4.

Visualizations—Visualizations of the cluster hierarchy plots and histograms were created in the R software environment. Correlation networks were visualized using TreeView software. Heatmaps were created using the ggplot2 package in R. Additional graphs were created using Prism (Graphpad).

Supplementary Material

Refer to Web version on PubMed Central for supplementary material.

Acknowledgments

We thank Professor Robert Tibshirani for critical reading of the manuscript. We also thank Angelica Trejo and Astraea Jager for technical support with the CyTOF and antibody labeling. B.G. is supported by the US National Institute of Health (T32GM089626) and the Stanford Society of Physician Scholars grant. G.K.F. is supported by the Stanford Bio-X graduate research fellowship and the US National Institute of Health (T32GM007276). R.V.B. is supported by the US National Institute of Health (5T15LM007033-27). S.C.B. is supported by the Damon Runyon Cancer Research Foundation Fellowship (DRG-2017-09) and US National Institutes of Health (1K99GM104148-01). This work was supported by grants from the US National Institutes of Health (UL1RR025744, 1R01CA130826, 5U54CA143907, HHSN272200700038C, N01-HV-00242, 41000411217, 1U19AI100627, P01 CA034233-22A1, U19 AI057229, U54CA149145, S10RR027582-01), the California Institute for Regenerative Medicine (DR1-01477, RB2-01592), the European Commission (HEALTH.2010.1.2-1), the US Food and Drug Administration (HHSF223201210194C: BAA-12-00118), the US Department of Defense (W81XWH-12-1-0591 OCRP-TIA NWC) and the Stanford Department of Anesthesiology, Perioperative and Pain Medicine.

References and Notes

1. Weiser TG, et al. An estimation of the global volume of surgery: a modelling strategy based on available data. Lancet. 2008 Jul 12.372:139. [PubMed: 18582931]
2. Kehlet H, Dahl JB. Anaesthesia, surgery, and challenges in postoperative recovery. Lancet. 2003 Dec 6.362:1921. [PubMed: 14667752]
3. Allvin R, Berg K, Idvall E, Nilsson U. Postoperative recovery: a concept analysis. Journal of advanced nursing. 2007 Mar.57:552. [PubMed: 17284272]
4. Lee L, Tran T, Mayo NE, Carli F, Feldman LS. What does it really mean to “recover” from an operation? Surgery. 2014 Feb.155:211. [PubMed: 24331759]
5. Bisgaard T, Stockel M, Klarskov B, Kehlet H, Rosenberg J. Prospective analysis of convalescence and early pain after uncomplicated laparoscopic fundoplication. The British journal of surgery. 2004 Nov.91:1473. [PubMed: 15386321]
6. DeCherney AH, Bachmann G, Isaacson K, Gall S. Postoperative fatigue negatively impacts the daily lives of patients recovering from hysterectomy. Obstetrics and gynecology. 2002 Jan.99:51. [PubMed: 11777510]
7. Bisgaard T, Klarskov B, Rosenberg J, Kehlet H. Factors determining convalescence after uncomplicated laparoscopic cholecystectomy. Arch Surg. 2001 Aug.136:917. [PubMed: 11485527]
8. Adamina M, Kehlet H, Tomlinson GA, Senagore AJ, Delaney CP. Enhanced recovery pathways optimize health outcomes and resource utilization: a meta-analysis of randomized controlled trials in colorectal surgery. Surgery. 2011 Jun.149:830. [PubMed: 21236454]
9. Stoecklein VM, Osuka A, Lederer JA. Trauma equals danger--damage control by the immune system. Journal of leukocyte biology. 2012 May 31.
10. Andersson U, Tracey KJ. HMGB1 is a therapeutic target for sterile inflammation and infection. Annual review of immunology. 2011; 29:139.
11. Rosenberger PH, et al. Surgical stress-induced immune cell redistribution profiles predict short-term and long-term postsurgical recovery. A prospective study. The Journal of bone and joint surgery. American volume. 2009 Dec.91:2783. [PubMed: 19952239]
12. Baigrie RJ, Lamont PM, Kwiatkowski D, Dallman MJ, Morris PJ. Systemic cytokine response after major surgery. The British journal of surgery. 1992 Aug.79:757. [PubMed: 1393463]
13. Bocsi J, et al. Modulation of the cellular and humoral immune response to pediatric open heart surgery by methylprednisolone. Cytometry. Part B, Clinical cytometry. 2011 Jul-Aug;80:212.
14. Hansbrough JF, Bender EM, Zapata-Sirvent R, Anderson J. Altered helper and suppressor lymphocyte populations in surgical patients. A measure of postoperative immunosuppression. American journal of surgery. 1984 Sep.148:303. [PubMed: 6236703]

15. Slade MS, Simmons RL, Yunis E, Greenberg LJ. Immunodepression after major surgery in normal patients. Surgery. 1975 Sep.78:363. [PubMed: 1098195]
16. Grossbard LJ, Desai MH, Lemeshow S, Teres D. Lymphocytopenia in the surgical intensive care unit patient. The American surgeon. 1984 Apr.50:209. [PubMed: 6370063]
17. Xiao W, et al. A genomic storm in critically injured humans. The Journal of experimental medicine. 2011 Dec 19.208:2581. [PubMed: 22110166]
18. Bone RC. Immunologic dissonance: a continuing evolution in our understanding of the systemic inflammatory response syndrome (SIRS) and the multiple organ dysfunction syndrome (MODS). Annals of internal medicine. 1996 Oct 15.125:680. [PubMed: 8849154]
19. Wilmore DW. From Cuthbertson to fast-track surgery: 70 years of progress in reducing stress in surgical patients. Annals of surgery. 2002 Nov.236:643. [PubMed: 12409671]
20. Liu T, et al. High dynamic range characterization of the trauma patient plasma proteome. Molecular & cellular proteomics : MCP. 2006 Oct.5:1899. [PubMed: 16684767]
21. Lin E, Calvano SE, Lowry SF. Inflammatory cytokines and cell response in surgery. Surgery. 2000 Feb.127:117. [PubMed: 10686974]
22. Reinke S, et al. Terminally differentiated CD8(+) T cells negatively affect bone regeneration in humans. Science translational medicine. 2013 Mar 20.5 177ra36.
23. Laudanski K, et al. Cell-specific expression and pathway analyses reveal alterations in trauma-related human T cell and monocyte pathways. Proceedings of the National Academy of Sciences of the United States of America. 2006 Oct 17.103:15564. [PubMed: 17032758]
24. Bjornson ZB, Nolan GP, Fantl WJ. Single-cell mass cytometry for analysis of immune system functional states. Current opinion in immunology. 2013 Aug.25:484. [PubMed: 23999316]
25. Bodenmiller B, et al. Multiplexed mass cytometry profiling of cellular states perturbed by small-molecule regulators. Nature biotechnology. 2012 Aug 19.
26. Bendall SC, Nolan GP, Roederer M, Chattopadhyay PK. A deep profiler's guide to cytometry. Trends in immunology. 2012 Jul.33:323. [PubMed: 22476049]
27. Bendall SC, Nolan GP. From single cells to deep phenotypes in cancer. Nature biotechnology. 2012 Jul 10.30:639.
28. Bendall SC, et al. Single-cell mass cytometry of differential immune and drug responses across a human hematopoietic continuum. Science. 2011 May 6.332:687. [PubMed: 21551058]
29. Maecker HT, McCoy JP, Nussenblatt R. Standardizing immunophenotyping for the Human Immunology Project. Nature reviews. Immunology. 2012 Mar.12:191.
30. Chan JK, et al. Alarmins: awaiting a clinical response. The Journal of clinical investigation. 2012 Aug 1.122:2711. [PubMed: 22850880]
31. Kehlet H, Wilmore DW. Multimodal strategies to improve surgical outcome. American journal of surgery. 2002 Jun.183:630. [PubMed: 12095591]
32. Christensen T, Bendix T, Kehlet H. Fatigue and cardiorespiratory function following abdominal surgery. The British journal of surgery. 1982 Jul.69:417. [PubMed: 7104617]
33. Finck R, et al. Normalization of mass cytometry data with bead standards. Cytometry. Part A : the journal of the International Society for Analytical Cytology. 2013 May.83:483. [PubMed: 23512433]
34. Ho CS, et al. Surgical and physical stress increases circulating blood dendritic cell counts independently of monocyte counts. Blood. 2001 Jul 1.98:140. [PubMed: 11418473]
35. Bruggner RV, Bodenmiller B, Dill DL, Tibshirani RJ, Nolan GP. Automated Identification of Stratifying Signatures in Cellular Sub-Populations. Accepted for publication Proc Natl Acad Sci U S A. 2014
36. Vuk-Pavlovic S, et al. Immunosuppressive CD14+HLA-DRlow/- monocytes in prostate cancer. The Prostate. 2010 Mar 1.70:443. [PubMed: 19902470]
37. Poschke I, Mougiakakos D, Hansson J, Masucci GV, Kiessling R. Immature immunosuppressive CD14+HLA-DR-/low cells in melanoma patients are Stat3hi overexpress CD80, CD83 and DC-sign. Cancer research. 2010 Jun 1.70:4335. [PubMed: 20484028]

38. Hoechst B, et al. A new population of myeloid-derived suppressor cells in hepatocellular carcinoma patients induces CD4(+)CD25(+)Foxp3(+) T cells. Gastroenterology. 2008 Jul. 135:234. [PubMed: 18485901]
39. Wakefield CH, Carey PD, Foulds S, Monson JR, Guillou PJ. Changes in major histocompatibility complex class II expression in monocytes and T cells of patients developing infection after surgery. The British journal of surgery. 1993 Feb.80:205. [PubMed: 8443652]
40. Tusher VG, Tibshirani R, Chu G. Significance analysis of microarrays applied to the ionizing radiation response. Proceedings of the National Academy of Sciences of the United States of America. 2001 Apr 24.98:5116. [PubMed: 11309499]
41. Park JM, et al. Signaling pathways and genes that inhibit pathogen-induced macrophage apoptosis--CREB and NF-kappaB as key regulators. Immunity. 2005 Sep.23:319. [PubMed: 16169504]
42. Beutler B. Inferences, questions and possibilities in Toll-like receptor signalling. Nature. 2004 Jul 8.430:257. [PubMed: 15241424]
43. Toshchakov V, et al. TLR4 but not TLR2, mediates IFN-beta-induced STAT1alpha/beta-dependent gene expression in macrophages. Nature immunology. 2002 Apr.3:392. [PubMed: 11896392]
44. O'Shea JJ, Plenge R. JAK and STAT signaling molecules in immunoregulation and immune-mediated disease. Immunity. 2012 Apr 20.36:542. [PubMed: 22520847]
45. Geijtenbeek TB, Gringhuis SI. Signalling through C-type lectin receptors: shaping immune responses. Nature reviews. Immunology. 2009 Jul.9:465.
46. Dai F, et al. Integration of pain score and morphine consumption in analgesic clinical studies. The journal of pain : official journal of the American Pain Society. 2013 Aug.14:767. [PubMed: 23743256]
47. Delogu G, et al. Apoptosis and surgical trauma: dysregulated expression of death and survival factors on peripheral lymphocytes. Arch Surg. 2000 Oct.135:1141. [PubMed: 11030869]
48. Giannoudis PV, et al. Immediate IL-10 expression following major orthopaedic trauma: relationship to anti-inflammatory response and subsequent development of sepsis. Intensive care medicine. 2000 Aug.26:1076. [PubMed: 11030163]
49. Lyons A, Kelly JL, Rodrick ML, Mannick JA, Lederer JA. Major injury induces increased production of interleukin-10 by cells of the immune system with a negative impact on resistance to infection. Annals of surgery. 1997 Oct.226:450. [PubMed: 9351713]
50. Nelson DE, et al. Oscillations in NF-kappaB signaling control the dynamics of gene expression. Science. 2004 Oct 22.306:704. [PubMed: 15499023]
51. Docke WD, et al. Monocyte deactivation in septic patients: restoration by IFN-gamma treatment. Nature medicine. 1997 Jun.3:678.
52. Hershman MJ, Cheadle WG, Wellhausen SR, Davidson PF, Polk HC Jr. Monocyte HLA-DR antigen expression characterizes clinical outcome in the trauma patient. The British journal of surgery. 1990 Feb.77:204. [PubMed: 2317682]
53. Hotchkiss RS, Opal S. Immunotherapy for sepsis--a new approach against an ancient foe. The New England journal of medicine. 2010 Jul 1.363:87. [PubMed: 20592301]
54. Makarenkova VP, Bansal V, Matta BM, Perez LA, Ochoa JB. CD11b+/Gr-1+ myeloid suppressor cells cause T cell dysfunction after traumatic stress. J Immunol. 2006 Feb 15.176:2085. [PubMed: 16455964]
55. Condamine T, Gabrilovich DI. Molecular mechanisms regulating myeloid-derived suppressor cell differentiation and function. Trends in immunology. 2011 Jan.32:19. [PubMed: 21067974]
56. Hall GM, Peerbhoy D, Shenkin A, Parker CJ, Salmon P. Relationship of the functional recovery after hip arthroplasty to the neuroendocrine and inflammatory responses. British journal of anaesthesia. 2001 Oct.87:537. [PubMed: 11878721]
57. Dhabhar FS, Malarkey WB, Neri E, McEwen BS. Stress-induced redistribution of immune cells--from barracks to boulevards to battlefields: a tale of three hormones--Curt Richter Award winner. Psychoneuroendocrinology. 2012 Sep.37:1345. [PubMed: 22727761]
58. Gurtner GC, Werner S, Barrandon Y, Longaker MT. Wound repair and regeneration. Nature. 2008 May 15.453:314. [PubMed: 18480812]

59. Murphy TJ, Paterson HM, Mannick JA, Lederer JA. Injury, sepsis, and the regulation of Toll-like receptor responses. Journal of leukocyte biology. 2004 Mar.75:400. [PubMed: 14557385]
60. Handy JM, et al. HLA-DR expression and differential trafficking of monocyte subsets following low to intermediate risk surgery. Anaesthesia. 2010 Jan.65:27. [PubMed: 19889110]
61. Ditschkowski M, et al. HLA-DR expression and soluble HLA-DR levels in septic patients after trauma. Annals of surgery. 1999 Feb.229:246. [PubMed: 10024107]
62. Tarnok A, et al. Preoperative prediction of postoperative edema and effusion in pediatric cardiac surgery by altered antigen expression patterns on granulocytes and monocytes. Cytometry. 2001 Aug 15.46:247. [PubMed: 11514959]
63. Degos V, et al. Depletion of bone marrow-derived macrophages perturbs the innate immune response to surgery and reduces postoperative memory dysfunction. Anesthesiology. 2013 Mar. 118:527. [PubMed: 23426204]
64. Bellamy N, Buchanan WW, Goldsmith CH, Campbell J, Stitt LW. Validation study of WOMAC: a health status instrument for measuring clinically important patient relevant outcomes to antirheumatic drug therapy in patients with osteoarthritis of the hip or knee. The Journal of rheumatology. 1988 Dec.15:1833. [PubMed: 3068365]
65. Ware JE Jr. SF-36 health survey update. Spine. 2000 Dec 15.25:3130. [PubMed: 11124729]
66. Beck AT, Steer RA. Internal consistencies of the original and revised Beck Depression Inventory. Journal of clinical psychology. 1984 Nov.40:1365. [PubMed: 6511949]
67. Paddison JS, Sammour T, Kahokehr A, Zargar-Shoshtari K, Hill AG. Development and validation of the Surgical Recovery Scale (SRS). The Journal of surgical research. 2011 May 15.167:e85. [PubMed: 21392804]
68. Jensen MP, Chen C, Brugger AM. Interpretation of visual analog scale ratings and change scores: a reanalysis of two clinical trials of postoperative pain. The journal of pain : official journal of the American Pain Society. 2003 Sep.4:407. [PubMed: 14622683]

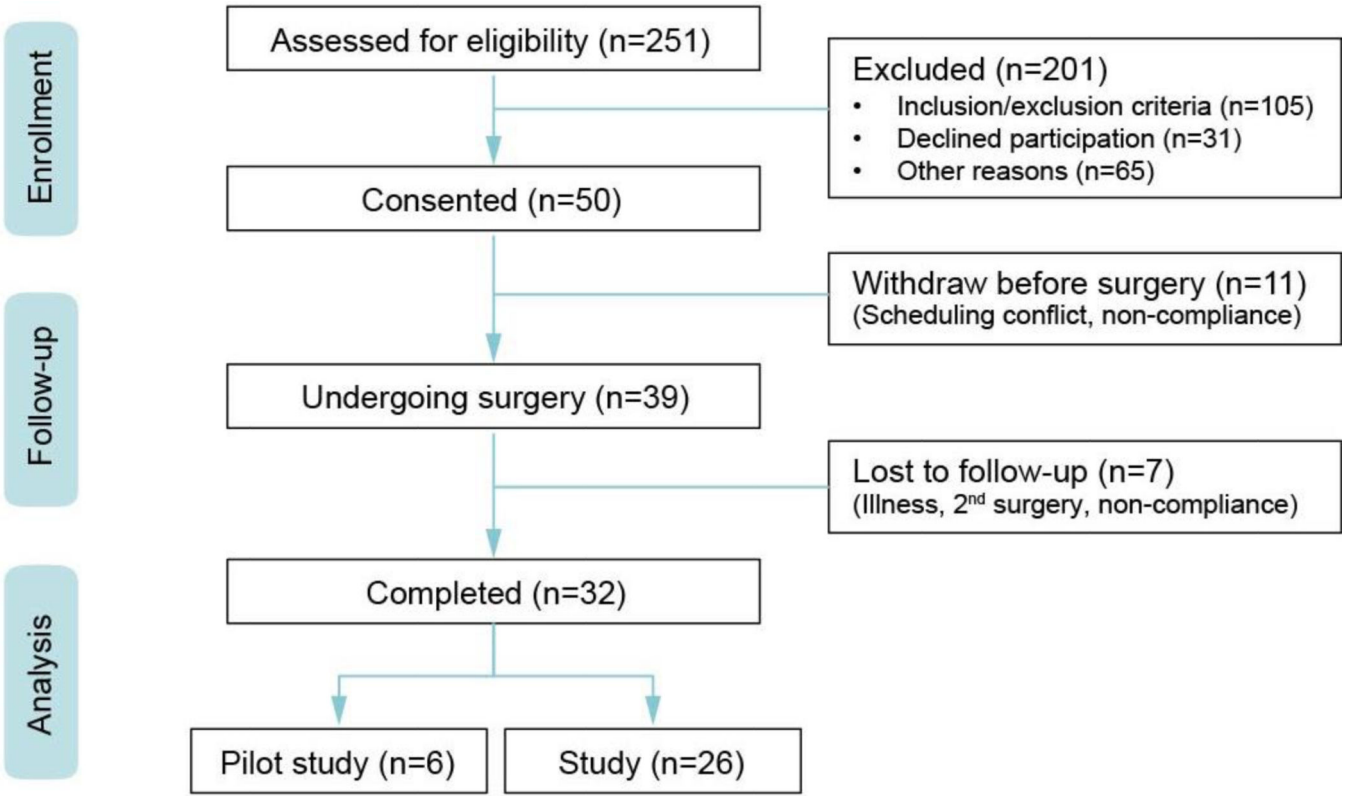

Fig. 1. Consort chart summarizes patient recruitment

Two hundred and fifty-one patients were assessed for eligibility, 50 were consented, 39 underwent total hip arthroplasty under the approved protocol, and 32 completed the study. Six patients were included in the pilot study, and 26 patients were included in the main study.

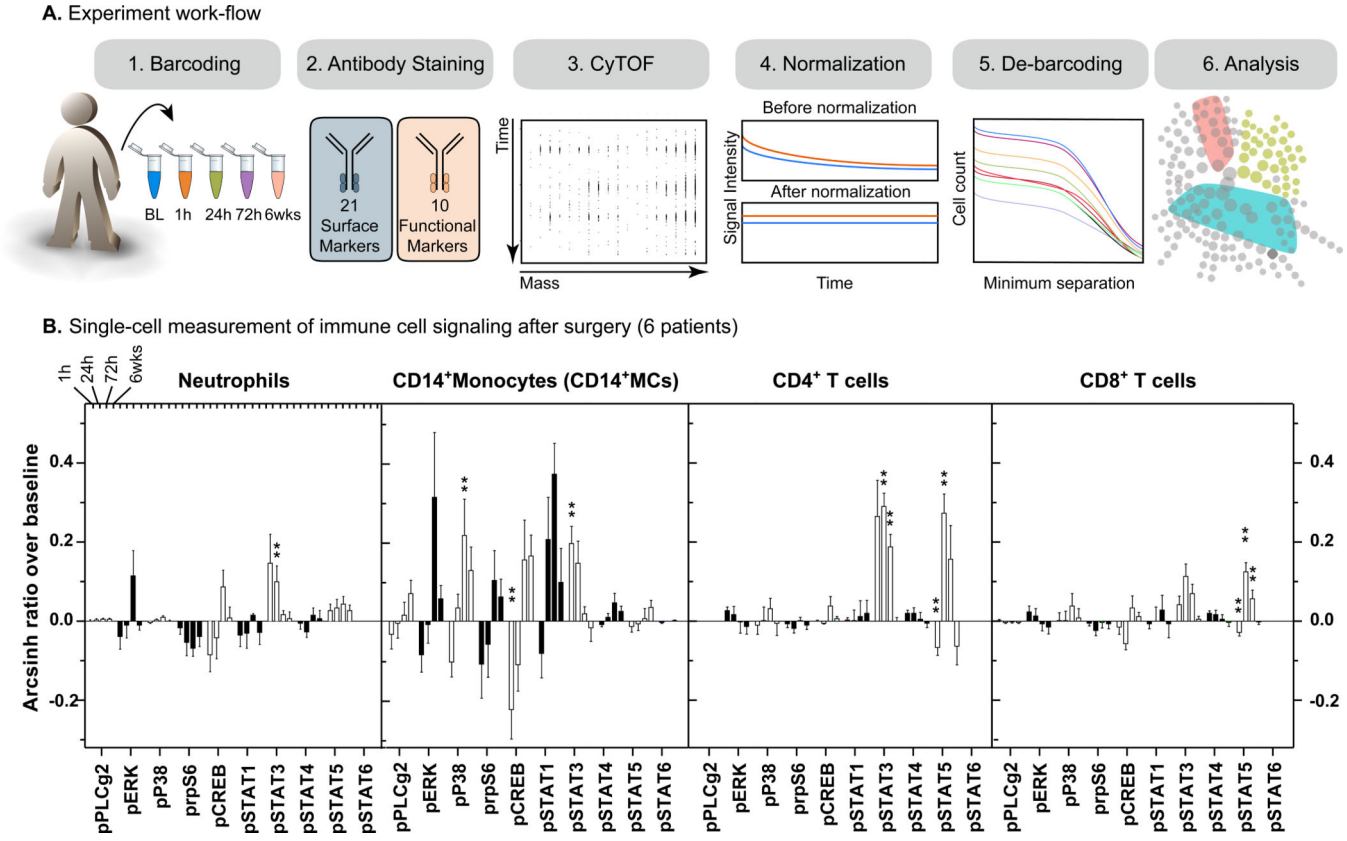

Fig. 2. Mass tag barcoding enables the longitudinal analysis of the cellular immune response in peripheral blood of patients undergoing surgery

A. Experimental workflow. Whole blood samples from six patients undergoing primary hip arthroplasty were collected 1 h before surgery (baseline, BL), and 1 h, 24 h, 72 h, and 6 weeks after surgery. Following red blood cell lysis, leukocyte samples from each patient were barcoded using a unique combination of palladium isotopes (*panel 1*). Barcoded samples were pooled, stained with a panel of 31 antibodies (*panel 2*, Table S1), and analyzed by mass cytometry (panel 3). Raw mass cytometry data were normalized for signal variation over time (33) (panel 4), de-barcoded (25) (*panel 5*) and analyzed (*panel 6*).

B. Assay validation in surgical patients. Ten intracellular signaling responses to surgery were quantified for four immune cell subsets (neutrophils, $CD14^+$ MCs, $CD4^+$ and $CD8^+$ T cells). Signal induction for each signaling molecule was calculated as the difference of inverse hyperbolic sine medians between samples obtained at baseline and at 1 h, 24 h, 72 h, and 6 weeks after surgery ("arcsinh ratio"). Five of 10 phospho-proteins (pSTAT1, pSTAT3, pSTAT5, pCREB, pP38) displayed reproducible changes at 1 h, 24 h, or 72 h after surgery compared to baseline. Results are shown as means ± SEM. SAM Two class paired was used for statistical analysis (** indicates a false discovery rate $q < 0.01$).

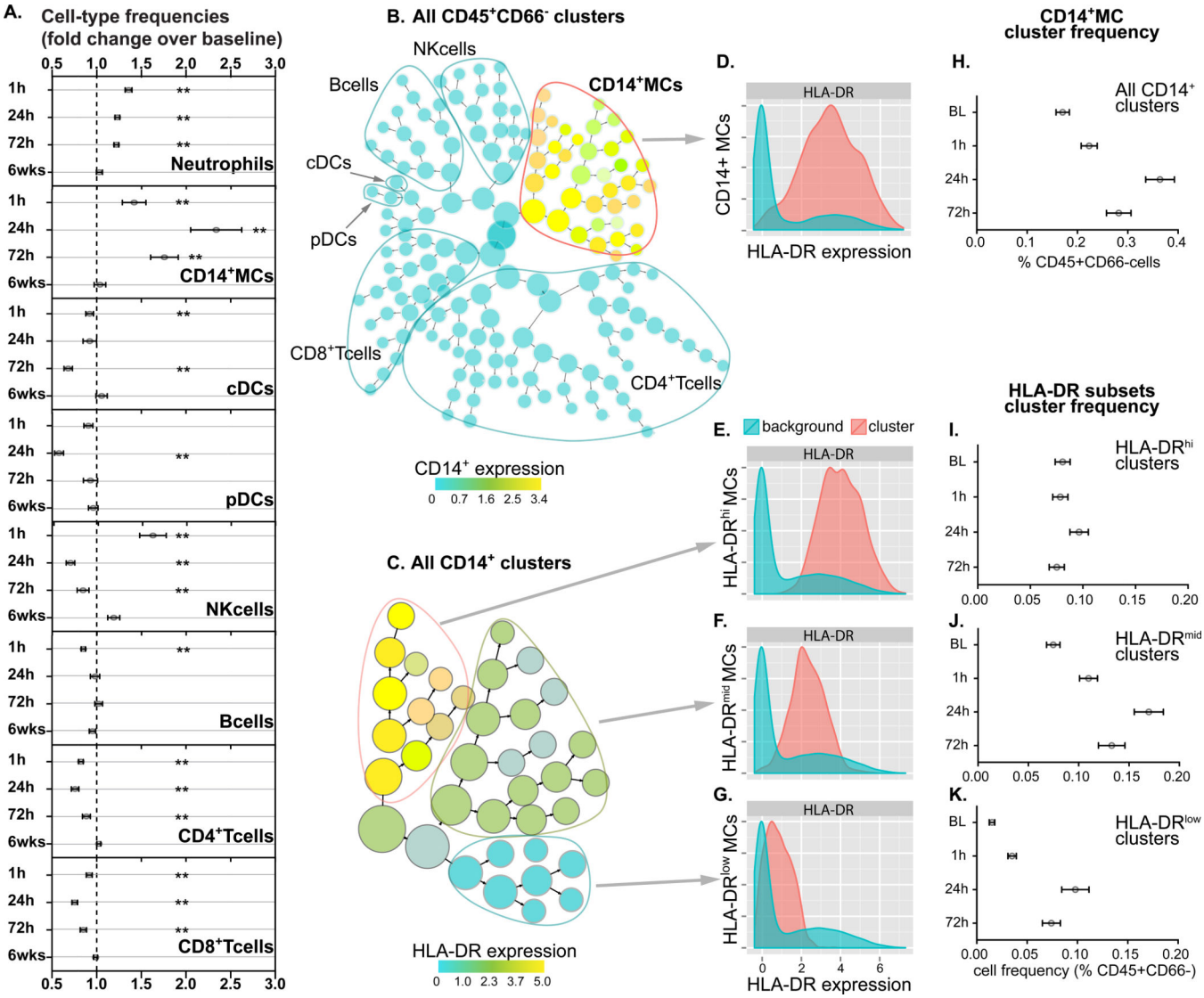

Fig. 3. Surgery induces a redistribution of major immune cell-types and a 6-fold expansion of HLA-DR^{low} CD14^{+} monocytes

A. Frequencies of neutrophils, CD14^{+} MCs, cDCs, pDCs, NK cells, B cells, CD4^{+} T cells, and CD8^{+} T cells are depicted for 26 patients 1 h, 24 h, 72 h, and 6 weeks after surgery. Cell-types were identified by manual gating (Fig. S2). Neutrophil frequency was quantified as percent of total hematopoietic cells (CD61CD235). All other cell frequencies are expressed as percent total of mononuclear cells (CD45^{+}CD66). Significant changes occurred for all cell types (**q<0.01, SAM Two class paired). Results are shown as mean fold change (± SEM).

B. Visual representation of unsupervised hierarchical clustering. Results are shown for CD45^{+}CD66 immune cells. The analysis used 21 cell surface markers (Table S1). Major immune cell compartments are contoured (Fig. S4). Contoured in red are CD14^{+} MCs. The color scale indicates median intensity of CD14 expression.

C. CD14^{+}MCs were clustered into HLA-DR^{hi} (yellow), HLA-DR^{mid} (green), and HLA-DR^{low} (blue) subsets. The color scale indicates the median intensity of HLA-DR expression.

D-G. Histogram plots. Arrows designate histograms of HLA-DR expression for $CD14^{+}$MC clusters (red) against HLA-DR background expression in all $CD45^{+}CD66^{-}$ cells (blue). *H-K.* $CD14^{+}$MC cell cluster frequencies 1 h before and 1 h, 24 h, and 72 h after surgery. Expansion of all $CD14^{+}$MC clusters (*H*) was attributable to the expansion of the HLA-DR^{mid} (*J*) and HLA-DR^{low} (*K*) $CD14^{+}$MC clusters. Results are shown as mean fold change (± SEM).

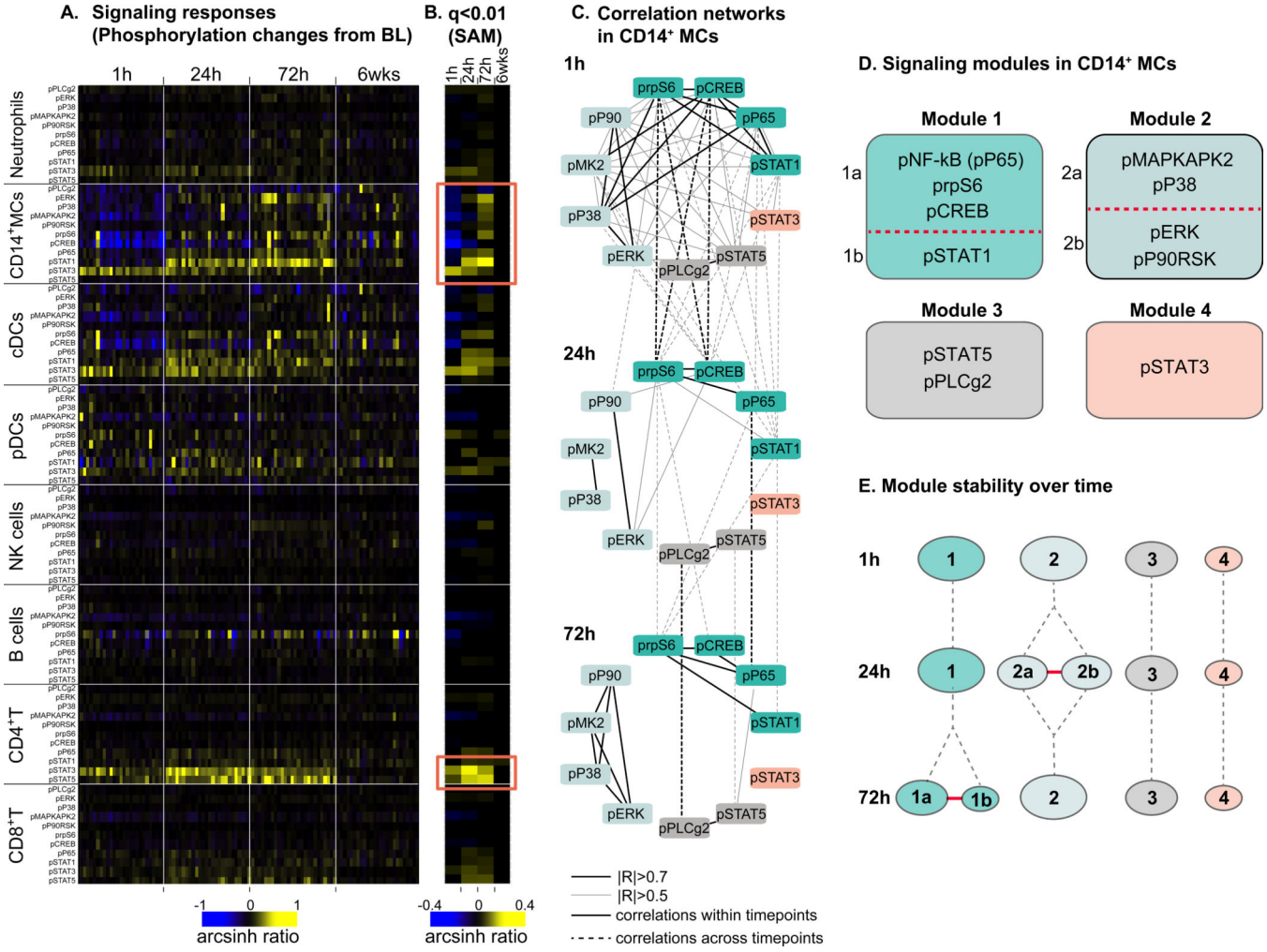

Fig. 4. Surgery induces time-dependent and cell-type specific activation of immune signaling networks

A. A heat map depicting hand-gated major immune cell subsets (rows, Fig. S2) and sampling times after surgery (columns). Within each block, changes in phosphorylation state of 11 intracellular signaling proteins (y-axis) are individually depicted for 26 patients (x-axis). The color scale indicates changes in phospho-signal median intensity (arcsinh ratio) compared to baseline.

B. Heat map depicting for each signaling protein, cell subset, and time point whether phosphorylation signals significantly increased (yellow, q<0.01, SAM Two class paired), decreased (blue, q<0.01), or remained unchanged (black, q>0.01). The color scale indicates mean fold-change of the signaling responses compared to baseline. Signaling responses in CD14^{+}MCs and CD4^{+} T cells were most prominent (red).

C. Pearson correlation coefficients between changes in phosphorylation states of 11 signaling proteins in CD14^{+}MCs at 1 h, 24 h, and 72 h after surgery were determined. Correlations within each (solid lines) and across (dash lines) time point(s) are depicted as black (|R|>0.7) and gray lines (|R|>0.5).

D. Signaling modules in CD14^{+}MCs at 1 h, 24 h, and 72 h were identified by cutting the dendrograms of clustered correlation coefficients (Fig. S7) using a threshold of R>0.7.

E. At 72 h, module 1 split into modules 1a (pNF-κB, prpS6, pCREB) and 1b (pSTAT1) that correlated with each other (R=0.46, red line). At 24 h, module 2 split into modules 2a (pMAPKAP2, pP38) and 2b (pERK, pP90RSK) that correlated with each other (R=0.45, red line).

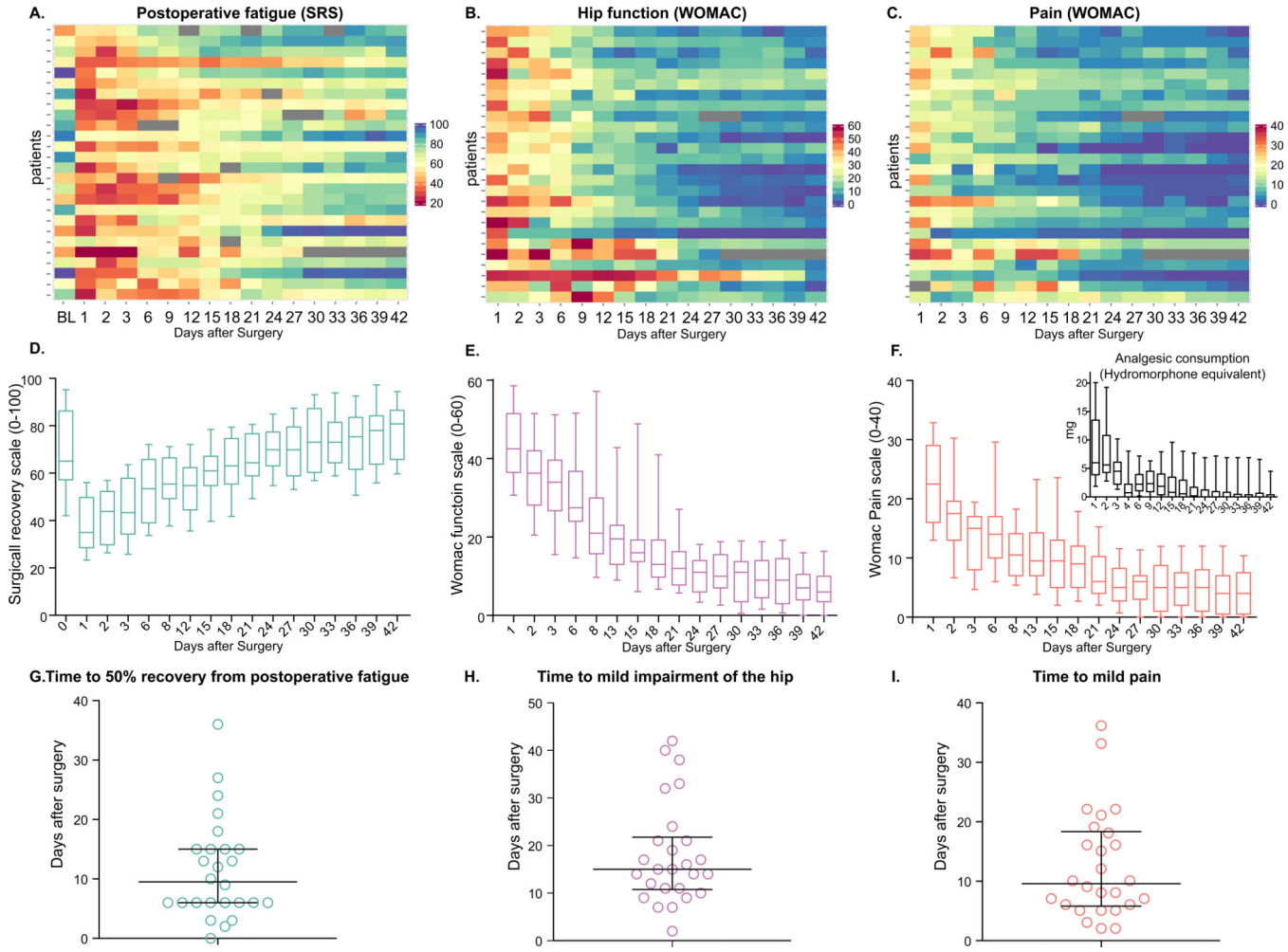

Fig. 5. The rate of surgical recovery varies greatly among patients

A-C. Heat maps depict the recovery parameters (*A*) postoperative fatigue, (*B*) hip function, and (C) pain for individual patients over the 6-week observation period. Postoperative fatigue was assessed with the Surgical Recovery Scale (SRS; 0–100 = worst-best function) (67). Pain and impairment of hip function were assessed with adapted versions of the Western Ontario and McMaster Universities Arthritis Index (WOMAC, pain 0–40 = no pain-worst imaginable pain; function 0–60 = no impairment-severe functional impairment) (64). The heat maps reflect significant variability for extent and rate of recovery across all three outcome domains.

D-F. Box plots depict medians and interquartile ranges of (*D*) SRS, (E) WOMAC function, and (*F*) WOMAC pain scores (bars indicate 10^{th} and 90^{th} percentiles). An inset graph in panel f depicts the median daily analgesic consumption expressed as the dose equivalent of intravenous hydromorphone. Graphical information regarding pain and analgesic consumption are jointly presented, as these variables are inter-dependent.

G-I. Clinical recovery parameters were derived to quantify rate of recovery for the three outcomes. Derived parameters were (*G*) time to 50% recovery from postoperative fatigue, (*H*) time to mild functional impairment of the hip, and (*I*) time to mild pain. Bars indicate median and interquartile range; open circles indicate individual data points.

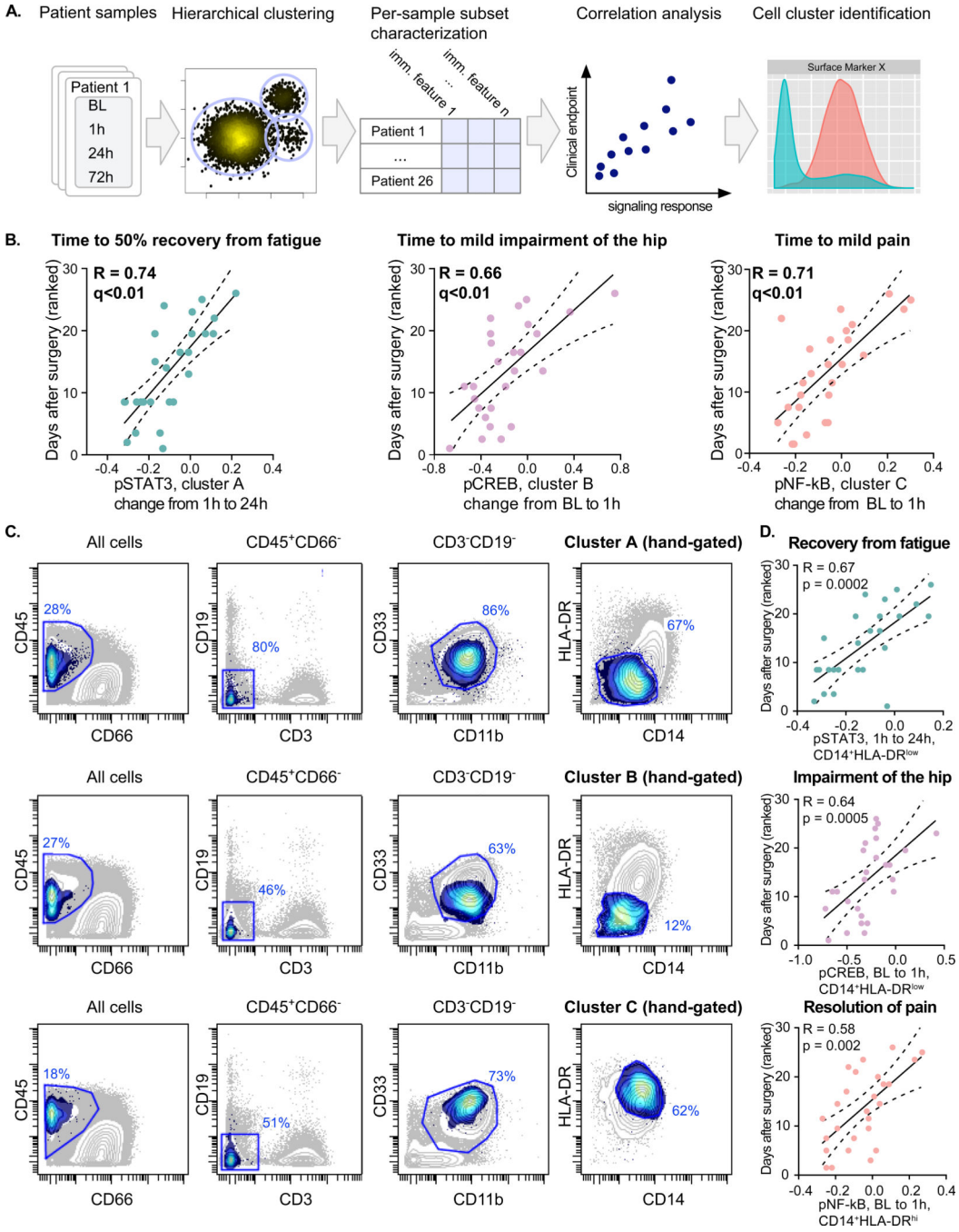

Fig. 6. STAT3, CREB, and NF-κB signaling in CD14$^+$MC subsets strongly correlate with surgical recovery

A. CD45$^+$CD66 cells obtained at BL and at 1 h, 24 h, and 72 h after surgery were clustered using an unsupervised approach (35) (*panels 1 and 2*, Fig. 3B). Immune features, which include frequencies and signaling responses of 11 phospho-proteins, were derived for every cluster (*panel 3*). SAM Quantitative was used to detect significant correlations between immune features and parameters of clinical recovery (q<0.01, *panel 4*). Cell cluster phenotypes were identified using cell surface marker expression (*panel 5*).

B. Significant correlations were obtained for STAT3 signaling in cluster A (*left panel*), CREB signaling in cluster B (*middle panel*), and NF-κB signaling in cluster C (*right panel*) with recovery from postoperative fatigue, functional impairment of the hip, and resolution of pain. Clusters A and B were $CD14^{+}HLA\text{-}DR^{low}$ MCs; cluster C was $CD14^{+}HLA\text{-}DR^{hi}$ MCs (Fig. S8).

C. Cells were hand-gated using 12 surface markers (blue line). Representative 2D plots are shown for one patient at 24 h (*upper panel*) and 1 h (*middle and lower panels*) after surgery. Percent cells in parent gate are shown. Cells contained in Clusters A, B, or C (*blue shadow*) are overlaid onto the entire cell population (gray).

D. Significant correlations between signaling responses and parameters of clinical recovery identified using an unsupervised approach were replicated with hand-gated data. Depicted are regression lines and 95% confidence intervals (*solid and dashed lines*), Spearman's ranked correlation coefficients, false discovery rates (q), and p-values.

Table 1

Demographic and clinical variables (n=26)

***Demographics*[1]**		
Gender (male/female)	16/10	
Race (Caucasian/African American)	25/1	
Age (year)	59.5 (54.0–68.0)	
Body mass index (kg/m^2)	26.5 (24.4–28.1)	
***Questionnaires*[2]**	***Before surgery***	***6 weeks after surgery***
SRS	62.3 (57.3–80.8)	80.8 (67.1–86.8)
WOMAC	131.5 (80.0–180.0)	33.5 (11.0–51.0)
SF36		
PCS	38.9 (21.9–42.1)	41.5 (31.1–49.8)
MCS	55.3 (39.7–59.6)	60.3 (49.3–64.3)
BDI	7.5 (3.0–11.0)	5.5 (1.0–8.0)
POMS-A		
Men	5.5 (3.5–9.5)	5.0 (4.0-6.8)
Women	7.0 (5.0–14.0)	4.0 (3.0–4.0)
Surgery		
Duration (min)	100 (85–119)	
Blood loss (ml)	250 (200–310)	
Urine output (ml)	200 (100–300)	
Fluids		
Crystalloids (ml)	1500 (1000–2000)	
Colloids (ml)	0 (0-0)	
Blood products (ml)	0 (0-0)	
Time to discharge (days)	3.1 (3.0–3.8)	
***Anesthesia*[3]**		
Technique		
General (number of patients)	6	
Spinal (number of patients)	1	
General + Spinal (number of patients)	19	
Volatile anesthetic		
Number of patients	25	
MAC (%)	0.5 (0.4–0.7)	
Nitrous oxide		
Number of patients	11	
MAC (%)	0.5 (0.4–0.6)	
Intrathecal medications		
Number of patients (%)	20	

Bupivacaine (mg)	11.3 (10.5–12.0)
Morphine (mg)	0.2 (0.1–0.2)
Opioid use[4]	
Intraoperative (mg)	2.8 (1.5–3.8)
During hospital stay (mg)	16.0 (13.1–27.4)
After discharge (mg)	9.0 (5.5–16.9)

1) Values indicate number of patients or median and interquartile range.

2) SRS = Surgical Recovery Scale (0–100, minimal to maximal general function); WOMAC = Western Ontario and McMaster Universities Arthritis Index (0–240; minimal and maximal joint impairment); SF36 = Short Form Health Survey; PCS = Physical Component Score (normalized average and standard deviation in general population = 50±10); MCS = Mental Component Score; BDI = Beck Depression Inventory (scores 0–13, 14–19, 20–28, and >28 = no, mild, moderate, and severe depression); POMS-A = Profile of Moods States Tension-Anxiety Scale (score > 10 for men and >16 for women are clinically significant).

3) MAC = Minimal Alveolar Concentration of average exposure during surgery.

Milligram equivalent of intravenous hydromorphone; Dose during hospitalization is total cumulative dose; Dose after discharge is cumulative dose taken on survey days (13 days during observation from day 6 to 42).

Table 2

Immune features correlating with clinical parameters of surgical recovery.

Clinical parameter	Immune feature type	Immune feature	Cell subset	R
Time to 50% fatigue	Signaling property	1h vs 24h cluster 519927 (A1), pSTAT3	$CD14^{+}HLA\text{-}DR^{mid}$	0.80
Time to 50% fatigue	Signaling property	1h vs 24h cluster 519972 (A), pSTAT3	$CD14^{+}HLA\text{-}DR^{low}$	0.74
Time to 50% fatigue	Signaling property	1hvs24h cluster 519978 (A2), pSTAT3	$CD14^{+}HLA\text{-}DR^{low}$	0.73
Time to 50% fatigue	Signaling property	1h vs 24h cluster 519805 (A3), pSTAT3	$CD14^{+}HLA\text{-}DR^{m,d}$	0.72
Time to mild pain	Signaling property	BLvs 1h cluster 519930 (C), pNFkB	$CD14^{+}HLA\text{-}DR^{h,}$	0.71
Time to mild Fl of the hip	Signaling property	BL vs 1 h cluster 519883 (B), pCREB	$CD14^{+}HLA\text{-}DR^{low}$	0.66

Significant immune features were cell abundance (percentage of total $CD45^{+}CD66$ cells) and signaling responses of eleven intracellular phospho-proteins within a cell cluster. Six significant correlations were detected between immune features and parameters of clinical recovery at a false discovery rate of $q<0.01$ (SAM Quantitative). Results are ranked by descending Spearman's correlation coefficients (R). All significant correlations were signaling responses in clusters within the $CD14^{+}$MC compartment. BL = base line, FI = functional impairment of the hip.